Size distribution and new particle formation in subtropical Eastern Australia

H. Guo[1*], A.J. Ding[1], L. Morawska[2], C. He[2], G. Ayoko[2], Y. S. Li[1], W. T. Hung[1]

1. Regional Air Quality, Department of Civil and Structural Engineering, The Hong Kong Polytechnic University, Hung Hom, Kowloon, Hong Kong
2. International Laboratory for Air Quality and Health, School of Physical and Chemical Sciences, Queensland University of Technology, Brisbane, Qld 4001, Australia

Environmental Context

Atmospheric submicrometer particles have significant impact on human health, visibility impairment, acid deposition and global climate. This study aims to understand the size distribution of submicrometer particles and new particle formation in Eastern Australia and the results indicate that photochemical reactions of airborne pollutants are the main mechanism of new particle formation. The findings will contribute to better understanding the effects of aerosols on climate and the reduction of submicrometer particles in the atmosphere.

Abstract

An intensive measurement campaign of particle concentrations, nitrogen oxides and meteorological parameters was conducted at a rural site in subtropical Eastern Australia during September 2006. The aim of this work was to develop an understanding of the formation and growth processes of atmospheric aerosols, and the size distributions under various meteorological conditions. In order to achieve this, the origins of air arriving at the site were explored using back trajectories cluster analysis and the diurnal patterns of particle number concentration and size distribution for the classified air masses were investigated. The study showed that photochemical formation of nucleation mode particles and their consequent growth was often observed. Further, the nucleation mode usually dominated the size distribution and concentration of the photochemical event in the first 3-4 hours with a geometric mean diameter of 26.9 nm and a geometric standard deviation of 1.28. The average

* Corresponding author. Tel: 852 3400 3962 Fax: 852 2334 6389 Email: ceguohai@polyu.edu.hk (Dr. H Guo)

particle growth rate was estimated to be 1.6 nm h^{-1}, which is lower than that observed at urban sites, but comparable to the values reported in clean environments. The potential precursors of the photochemical events are also discussed.

Key words: New particle formation; Particle growth rate; Particle size distribution; Photochemical event; Back trajectory

1. Introduction

Submicrometer particles in the atmosphere (< 1 μm in diameter) have attracted much research interest in scientific community due to their impact on human health, visibility impairment, acid deposition and global climate [1-5]. These particles normally contain trace elements and toxins, and have a very high probability of depositing deep in the respiratory tract, owing to the high diffusion coefficients of the particles [6].

Sulfuric acid is one of primary precursor species of newly formed particles with diameter of 3-4 nm [5]. Particles with a diameter range of 50-200 nm are climatically relevant, as particles in the range can act as cloud condensation nuclei (CCN) [7-9]. The number of particles present when a cloud forms affects the size of the resulting cloud droplets and the radiative properties of the cloud. Thus, particles have an indirect impact on climate [10]. On the other hand, particles with a diameter range of 100-800 nm scatter and absorb incoming solar radiation efficiently and alter the radiative properties of the Earth's atmosphere directly. As a result they have a direct impact on the climate. In addition, particles with diameters similar to the wavelengths of visible light (400-700 nm) are particularly effective in light scattering [1], leading to reductions in visibility.

Typically, the size distribution of submicrometer particles has a tri modal structure: a nucleation mode, representing quite recently formed particles, along with Aitken and accumulation modes, representing aged particles [11]. The nucleation mode particles result from the chemical conversion of gases to low volatility vapors, and they usually range in size from 1.5 to 30 nm [9, 12-16]. The Aitken mode particles are generated from the condensation of low vapor pressure substances and gas-to-particle conversion, and they usually range in size from 20 to 130 nm [13, 15, 17]. These particles may also be directly emitted from combustion processes, such as vehicular emissions, especially from diesel engines. The accumulation mode particles, on the other hand, grow from Aitken particles through the process of coagulation and condensation, and they usually range in size from 100 to 1000 nm [12-13, 15, 18]. These three size modes are observed to be present at variable mean diameters in different locations and large variations exist in the data from different locations.

Since the 1990s, many measurements have been conducted to study the size distribution and new particle formation within the submicrometer particles in the northern hemisphere.

Some examples include: the International Arctic Ocean Expedition 1991 (IAOE-91) [12, 18]; field measurements at Idaho Hill and Mauna Loa Observatory [5, 19-20]; studies conducted in background stations in Antarctica, Finnish Lapland and Boreal Forest stations, as well as in polluted urban sites in Greece and India [17, 21-24]; the SATURN experiment in Germany [9]; the Supersite studies in the United States [25-27]; and the PRD study in southern China [15]. In the southern hemisphere, however, few studies have been carried out in urban and suburban/rural areas of Australia, where the total anthropogenic emissions of air pollutants are much lower, due to lower overall population densities (a total of 10 to 12% of the human population), lower levels of industrialisation and smaller land masses. Suni et al. [28] studied the formation and characteristics of ions and charged aerosol particles in a native Australian Eucalypt forest, whereas Jimi et al. [29] reported the sources and concentrations of newly formed nanoparticles in an Australian Baseline Air Pollution Station. Both studies claimed that new particle formation in Australia is largely natural.

In order to gain insight into the formation and growth processes of atmospheric aerosols, and the size distributions under the meteorological conditions observed in subtropical Eastern Australia, an intensive real-time measurement data of particle number concentrations, along with simultaneously measured nitrogen oxides (NOx) and meteorological parameters, is presented.

Brisbane, the capital city of Queensland, Australia, lies in the south eastern region of the state, at approximately 27˚30'S and 153˚06'E. The southeast Queensland region has a population of approximately 1.77 million, with both a small industrial base and an extended residential area [30]. The populated area extends approximately 40 km along the coastline to the north and south of Brisbane, and 35 km west to the city of Ipswich. The topography of the surrounding area is moderately complex, with the start of a mountain range (230 m elevation) 10 km to the west of the city and heading in a northwesterly direction. The range then goes on to exceed 700 m elevation approximately 35 km from the city center, and this scarp is used to define the western edge of the air shed. Other mountain ranges, with peaks above 1000 m, lie to the south of the region and define the southern boundary of the air shed.

Wind flows in the region are governed by synoptic flows, which are most often from the southeast, with a period of strong westerly flows lasting for one or two months during the

97 winter. A northeasterly sea breeze is a daily feature throughout the year, with an overnight
98 southwesterly drainage flow from the mountain range to the west, which carries air parcels
99 from the plateau region and the western coastal plain towards the city. However, under more
100 rare conditions, that give rise to gradient winds from the northwest, the combination of the
101 light synoptic northwesterly flow and the overnight southwest drainage flow can delay the
102 onset of the sea breeze, causing the recirculation of the city emissions, leading to
103 photochemical smog events.
104
105 **2. Methods**
106 2.1. Measurement site
107 The measurement site was located approximately 35 km southeast of Brisbane (27˚45'S,
108 153˚06'E), and it was surrounded by a small town, bush land and agricultural areas. The
109 nearest road is 400 m to the east, carrying a low level of local traffic (<10 vehicles per hour).
110 Between the national highway and the measurement site, there are large areas of forests
111 (Figure 1a).
112 The intensive sampling campaign was conducted in spring 2006, between 4 – 26
113 September when the temperature ranged from 12.5 to 23.8˚C. September was chosen for the
114 measurement campaign because the meteorological conditions are generally favorable to the
115 photochemical reactions. For example, average hours of sunlight per day are the highest (9
116 hours), whereas the average monthly rainfall is the lowest (35 mm) throughout the year [31]. In
117 addition, biomass burning is often practiced in the forest areas and the farming land during
118 spring, when the wind speed is usually relatively light.
119 Continuous measurements of particle number concentrations, together with
120 meteorological conditions and gaseous pollutants, were conducted at the site by
121 instrumentation installed and operated in an air-conditioned trailer. Ambient air, from
122 approximately 2 m above the ground, was drawn into the instrumentation via 1.5 m long
123 conductive plastic tubes, with an inner diameter of 8 mm, from an inlet on the roof of the
124 trailer, and losses in the inlet tube were estimated based on laminar flow diffusion theory [32].
125
126 2.2. Measurements of particle number concentration

Particle number concentration and size distribution in the size range 15 to 737 nm were continuously measured using an automated, software controlled Scanning Mobility Particle Sizer (SMPS), comprising of an Electrostatic Classifier (EC) (TSI, Model 3071A) and Condensation Particle Counter (CPC) (TSI Models 3010). The SMPS operates on the principle of particle classification by the EC according to the electrical mobility of the particles, which is a function of their size, followed by particle counting by the CPC, which utilises laser light scattering to count the particles. The ratio of aerosol/sheath air flow for the EC was kept at 1/10 (0.3 l/min to 3 l/min), and the scan time was three minutes.

2.3. Measurements of meteorological parameters and nitrogen oxides concentrations

Continuous measurements of meteorological parameters and NOx concentrations were carried out during the sampling campaign. Total solar radiation, wind direction, wind speed, air temperature and relative humidity were measured by a portable weather station (Davis Instruments Weather Monitor II), with temperature and relative humidity measured 1.8 m above the ground, and wind direction and wind speed measured at a height of 4 m.

Ambient NO, NO_2, and NO_x concentrations were also measured on a continuous basis by a chemiluminescence based nitrogen oxides analyser (Model 9841A, Ecotech), with a time resolution of 4 seconds.

2.4. Calculation of backward trajectories

In order to develop an understanding of the possible influence of long-range transport on the particles, as well as particle formation and growth, 2-day backward trajectories were calculated for each sampling hour, using the HYSPLIT model (Hybrid Single Particle Lagrangian Integrated Trajectory, Version 4.8) from NOAA Air Resources Laboratory (http://www.arl.noaa.gov/ready/hysplit4.html). The model was driven by NCEP Global Data Assimilation System (GDAS) output, which has a horizontal resolution of 1 x 1 degree in latitude and longitude, 23 vertical sigma levels and a 3 hour temporal resolution (for details about the data please refer to http://www.arl.noaa.gov/ss/transport/gdas1.html). Using the trajectory cluster analysis function of HYSPLIT, all backward trajectories (for each hour

during the experiment period) were classified into four groups, based on the location of air in the initial 24 hours for each trajectory.

2.5. Definition of a particle formation event

The definition of a particle formation event was formulated based on the criteria described by Birmili and Wiedensohler [33] and Mäkelä et al. [22]. However, the distinction between a particle formation event and a non-event is difficult and somewhat subjective since the number of nucleated particles may be relatively small when compared to the number of background particles. In this study, an event is assumed to have taken place if there is a clear increase in the number of nucleation mode particles, in the absence of any anthropogenic source emissions, followed by their growth over a period of several hours.

Since the smallest particle that can be measured by the SMPS was 15 nm in diameter, we were unable to see the particles when they first nucleated, as the typical diameter of a nucleated molecular cluster is around one nanometer. As such, when the particles were actually detected, they would have already grown from their initial size. However, since growth rates of the order of several nanometers per hour are usually observed, the particles detected in this study were still relatively new. In addition, the evolution towards larger particle sizes in the particle size spectra, during the particle formation process, is always interpreted as a particle growth process.

3. Results and discussion

3.1. Characteristics of air masses from different regions

3.1.1. Classification of air masses

Figure 1b shows the average trajectory pathways of the four clusters during the entire study period. The three major air clusters, being inland air (cluster 1), marine air (cluster 2) and marine plus local air (cluster 3), were well defined, with the inland air masses (cluster 1) accounting for 17% of the total air samples. These air masses arrived at the sampling site from a southwesterly direction, passing through several agriculturally areas and small towns. On the other hand, the marine air (cluster 2) accounting for 34% of the total air samples. These air masses originated from the ocean located in a southeast-south direction from the measurement

site and were transported rapidly to the sampling site. Finally, the cluster 3 air masses (38%), originating from the ocean, were slowly transported to the measurement site at lower wind speeds, originating from southeast-east directions. Therefore, these air masses were affected by local sources present to the east and southeast of the measurement site. As such, air from both clusters 2 and 3 could be influenced by the forests and vehicular sources they encountered during their transport to the sampling site, however such influences are likely to be more prevalent in cluster 3, which was transported more slowly than the cluster 2 air.

In addition, it can be seen that approximately 11% of the air masses originated from the ocean, traveled towards the continent in westerly direction and then turned to approach the site from the north (marine plus urban - cluster 4). During transport, these air masses were likely to have passed through Brisbane city, and therefore, they may have been influenced by urban emissions, in addition to local sources.

3.1.2. Particle size distribution of classified air masses

Figure 2 presents contour plots of the average diurnal variations in particle size distribution for the three typical air masses, along with meteorological data and the concentrations of gaseous pollutants during the entire study period. Here, the cluster 4 air (marine plus urban) was not presented, as it accounted for only 11% of the total air masses. However, given that a photochemical event was observed on 20 September 2006, and that the major air mass identified was cluster 4 air, the results for cluster 4 are therefore discussed in detail as a case of photochemical particle formation in Section 3.2.1. Since different sized particles have different sources and formation routes, as well as physical and chemical characteristics, the size spectra analysis indicates that the submicrometer particles can be categorised into three modes: Dp < 30 nm (nucleation mode), 30 – 100 nm (Aitken mode), and Dp > 100 nm (accumulation mode). Thus, the diurnal variations of the particle number concentrations are also shown for each of the three modes (Figure 2) and the average particle number concentrations and the time with the maximum value for each of the three modes in each cluster air mass are summarized (Table 1).

3.1.2.1. Inland air (cluster 1)

High number concentrations of Aitken mode and accumulation mode (maximum concentration for Aitken mode and accumulation mode was approximately 4.0×10^3 and 2.2×10^3 cm^{-3}, respectively) were observed, beginning at approximately 6:00am, peaking at 7:00am and then disappearing subsequent to the break-up of the nocturnal inversion layer and the development of the daytime boundary layer, which favored the dispersion of air pollutants due to the increased height of the boundary layer (Figure 2).

This morning peak of Aitken and accumulation modes particles coincided with the morning peak of the gaseous pollutant NO, which is a good tracer of fresh combustion sources [14, 27]. The increased particle number and air pollutant concentrations observed in the morning are likely to be related to the traffic events and/or cooking activities of local residences near the sampling site. The NO_x ($NO + NO_2$) concentration ranged from 15 to 30 ppb during 6:00-8:00am, which was much lower than the values observed, for example, in Atlanta (~120 ppb), Fresno (~99 ppb) and Gwangju (60 ppb) [14, 25, 27]. This implies that the source strength at the sampling site was much less than that observed in the other studies, leading to lower particle number concentration in the event.

With the increase in solar radiation and temperature, along with the decrease in relative humidity during the morning (i.e. conditions typically attributed to clear days), the submicrometer size distribution showed a clear increase in the nucleation mode particle concentration during the late morning, followed by the subsequent growth of these particles into Aitken and accumulation mode sizes throughout the afternoon and evening, which persisted until the break-up of nocturnal inversion the next morning. The evolution of the size spectra illustrated the growth of the nucleation mode up to sizes in the range of 50 – 100 nm over periods of about 10 hours, which is consistent with the observations made in marine boundary layers [18], the free troposphere [34], coastal sites [35], the arctic boundary, Antarctica and boreal forests [17].

Furthermore, evening peaks of Aitken and accumulation mode particles, and NO in the inland air, were always observed around 18:00-19:00, representing the time period when local residents were most likely to be travelling and/or undertaking cooking activities. Overall, particle formation events caused by photochemical reactions often followed this very

246 distinctive pattern, and were observed throughout the entire sampling period, mostly on sunny
247 days. A detailed discussion on the formation and growth of these photochemically formed
248 particles is given in Section 3.2.
249
250 3.1.2.2. Marine air (cluster 2)
251 The same diurnal pattern as in clusters 1 was also found in cluster 2, however the
252 concentrations of the three mode particles were lower for cluster 2 (all below 1.0×10^3 cm^{-3}).
253 This was due to the strong southeasterly wind from the Tasman Sea, which brought clean
254 marine air and scattered rain to the sampling site, and diluted most of the airborne pollutants
255 generated by sub-regional and local sources. However, small peaks of Aitken mode particles
256 and NO were observed at approximately 7:00am, which were attributed to local traffic and/or
257 cooking activities.
258 Though particle formation events were also observed at midday, it was found that the
259 modal diameter and concentration of the newly formed (newly appeared) particles remained
260 unchanged between 12:00 and 15:00. This is different from the particle formation events
261 observed in clusters 1 and 3, and a possible interpretation for this phenomenon is as follows:
262 the speed of southeasterly winds was high (~3 m/s) during 12:00 – 15:00, and thus few
263 nucleation mode particles were produced during the transport of the air mass. The retention
264 time for the arrived air mass was only enough to generate nucleation mode particles via
265 photochemical reactions, but it was not sufficient for the generated nucleation mode particles
266 to grow larger before the old air mass was replaced by a fresh air mass. If this is true, higher
267 levels of larger particles (e.g. Aitken and accumulation modes) would be found somewhere
268 downwind of the site. In late afternoon and evening, reduced wind speed and temperature and
269 increased relative humidity led to the growth of larger particles, whereas the build-up of
270 inversion layer caused by radiation cooling of the ground resulted in the decrease in the height
271 of boundary layer which elevated concentrations of larger particles.
272
273 3.1.2.3. Marine air affected by local sources (cluster 3)
274 Compared to the particle number concentration of inland air (cluster 1), the particle
275 number concentration of cluster 3 air masses was 2-4 times lower (Figure 2). Similar to inland

air, the coinciding peaks of NO and Aitken mode particles which appeared in the early morning (6:00-7:00am) were mainly caused by local combustion sources (i.e. vehicular emissions and/or cooking activities), however, despite the source strength of these activities, particle concentration was often diluted by the clean marine air masses. On the other hand, in the late morning, a burst of nucleation mode particle concentrations was often found, which was followed by the growth into Aitken and accumulation mode particles, until the morning of next day, when the mixing layer was well developed.

3.1.2.4. Diurnal patterns of submicrometer particles in the classified air masses

In order to learn more about the characteristics of submicrometer particles in the three major air masses, the day time and night time particle size distributions of the three classified air masses were investigated (Figure 3). It can be seen that at night time (20:00-06:00), the particle size distribution was dominated by Aitken mode particles, with a GMD (geometric mean diameter) of 84 nm, 57 nm and 66 nm for cluster air 1, 2, and 3, respectively. These results are consistent with those observed in the tropospheric background in Finland [13], as well as in southern China [15]. During the night time, inland air had the highest total particle concentration (4.64×10^3 cm^{-3}), followed by marine air clusters 3 (2.99×10^3 cm^{-3}) and 2 (1.22×10^3 cm^{-3}).

In contrast, the day time particle size distribution presented different modal structures for the different air masses. The inland air showed a bimodal spectrum, which can be explained by the Aitken and accumulation modes (GMD: 32 nm and 116 nm, respectively), whereas a single modal distribution was found for marine air clusters 2 and 3, with a GMD of 20.6 nm and 28.9 nm, respectively. The size distribution observed in the three air clusters was found to be reasonably well related to photochemical formation patterns throughout the day, and the GMD of the smaller particles was comparable to that observed in East Asia [14-15], but slightly higher than that observed in southern Finland, Germany and the United States [5, 9, 13]. During the day time, total particle concentration in cluster 1 air was the highest (1.30×10^3 cm^{-3}), while cluster 2 air had the lowest particle concentration value (9.60×10^2 cm^{-3}). It can be seen that the particle concentration was generally higher at night than during the day, due to the impact of nocturnal inversion.

306 Overall, the particle number concentrations observed at this rural site were lower than
307 those observed in urban areas such as Brisbane [36], Atlanta [25], Pittsburgh [26] and Gwangju [15],
308 and were comparable to concentrations found in the Arctic, Antarctica, boreal forests [17] and a
309 clean continental site [5], they were slightly higher than that in the high-alpine site of
310 Jungfraujoch [37].
311
312 3.2. Photochemical formation of particles
313 In total, 7 new particle formation events were identified during the intensive sampling
314 period. The percentage occurrence of the events (~32%) was higher than that reported for
315 most locations such as Finland (~14 - 28%), Korea (~14%) and China (~25%) [14-15, 38-39], but
316 much lower than that observed at a background site in South Africa (over 90%) [40].
317
318 *3.2.1. Photochemical formation of nucleation particles*
319 An example of the data recorded for a photochemical event on 20 September in 2006 is
320 presented in Figure 4. Using trajectory cluster analysis, the air masses were found to have
321 been transported slowly from the north and northeast, probably passing over urban Brisbane,
322 indicating that this data was from a cluster 4 air mass (see Figure 1). This is consistent with
323 the wind data measured at the site. In the morning, solar radiation intensity and temperature
324 increased rapidly, and the wind speed increased from zero to light northerly winds, following
325 the break-up of the nocturnal inversion layer. The nucleation mode appeared in the
326 measurement range at about 11:00am and the nucleation mode particle concentration
327 increased rapidly from ~8.85×10^{2} cm^{-3} to 5.68×10^{3} cm^{-3} at noon. The nucleation and Aitken
328 modes shifted towards each other during the afternoon, until 15:00, as a result of the intensive
329 growth of the nucleation mode particles. The peak of Aitken mode particles correlated well
330 with the peak of nucleation mode particles, with a time delay of about one hour, suggesting
331 the growth of nucleation mode particles into Aitken mode particles. After 15:00, the total
332 particle number concentration decreased rapidly due to coagulation losses and a significant
333 reduction of solar radiation, leading to a significantly lower production of new particles.
334 Nucleation mode particle concentrations were anti-correlated with aerosol surface area
335 concentrations, i.e. lower nucleation mode particle concentrations were recorded during the

periods of higher aerosol surface area concentrations. This is consistent with the observations reported in other studies [5, 15], and can be attributed to the fact that concentrations of the nucleating species decrease due to heterogeneous condensation, as pre-existing aerosol concentrations increases, resulting in a reduction in particle production rates. Furthermore, the likelihood that a freshly formed nucleus grows to a detectable size before it is scavenged by the preexisting aerosol also decreases with increasing aerosol surface area concentrations [5].

The particle size distribution of the photochemical formation event observed at the site on 20 September in 2006 is illustrated in Figure 5. For the purpose of comparison, the size distribution of a biomass burning event is also shown in Figure 5. The biomass burning event was captured on 16 September between 1:00 – 10:00am, when wood was burnt 20m from the sampling site. The nucleation mode dominated the size distribution of the photochemical event, with a GMD of 26.9 nm and a geometric standard deviation (GSD) of 1.28. On the other hand, the biomass burning event showed a bimodal lognormal distribution, dominated by Aitken (GMD: 36.7 nm, GSD: 1.21) and accumulation (GMD: 58.4 nm, GSD: 1.14) modes. However, the total particle number concentration of the biomass burning (2.38×10^4 cm^{-3}) was much higher than that of the photochemical event (3.81×10^3 cm^{-3}), indicating the difference in source strength.

3.2.2. Potential precursors of nucleation mode particle formation

Previous studies have reported that the principle nucleation precursor species are sulfuric acid (H_2SO_4) and biogenic volatile organic compounds (BVOCs) [5, 28, 41]. However, it is hypothesised that the contribution of sulfuric acid to particle formation and growth might be substantially larger in urban environments than in most clean locations. This hypothesis is supported by comparing the results of Boy et al. [42] and Stanier et al. [26], which showed that H_2SO_4 is responsible for 10% and 100% of the particle formation and growth in remote forest and polluted environments, respectively [17]. However, Marti et al. [43] and Weber et al. [5] assessed the contributions of SO_2 and organic precursors at a remote continental site and concluded that sulfuric acid was probably responsible for most of the observed newly formed nucleation mode particles. They also found that whilst low-volatility organic compounds may have caused particle formation under the right conditions, they were more likely to condense

upon pre-existing particles.

In this study, SO_2 data was obtained from the Environmental Protection Agency of Queensland Government (http://www.epa.qld.gov.au), and statistical analysis indicated that, whilst average SO_2 concentrations in Brisbane are generally quite low, the hourly average SO_2 concentration on 20 September 2006 showed a good correlation with the concentration of nucleation mode particles (R^2 = 0.51, p = 0.0012), suggesting that SO_2 products might be involved in the increased nucleation mode particle concentration during this photochemical event. This is consistent with the recent work of Suni et al. [28] in an Australian forest where SO_2 was suggested to make a significant contribution to nucleation precursors. It is also comparable to the observations made during photochemical events in Atlanta [25], the Rocky Mountains [43] and Gwangju [14].

The average SO_2 concentration in this photochemical event (< 1ppb) was much lower than that observed in Atlanta (4-12 ppb) and Gwangju (~2.5 ppb) [14, 25]. Similarly, the average concentration of nucleation mode particles observed during this event (~3.0 × 10^3 cm^{-3}) was also much lower than that found in both Atlanta and Gwangju [14, 25], which is likely to be the result of the lower SO_2 products (i.e. H_2SO_4) present. However, since there are also forests near the sampling site, which would emit biogenic VOCs (i.e. isoprene and monoterpenes) during high temperatures and strong solar radiation, the possibility that BVOCs were associated with the increase in nucleation mode particle concentrations during the photochemical event can not be excluded. Thus, more research is required, in order to understand the relationship between SO_2, BVOCs and the formation of nucleation mode particles.

3.2.3. Particle growth rate

Particle diameter growth rate (dDp/dt in nm h^{-1}) was estimated by calculating the evolution of GMD for the modal mode as a function of time during the photochemical event (Figure 6). It can be seen that the initial particle size and the average particle growth rate on 20 September 2006 were 3.69 nm and 1.6 nm h^{-1}, respectively. This growth rate is lower than the values measured for urban sites such as Gwangju (2.2 – 4.7 nm h^{-1}), Atlanta (2.86 – 22.02 nm h^{-1}) and St. Louis (6.7 nm h^{-1}) [14, 44-45], but is comparable to those observed in Antarctica

396 (0.3 – 2.7 nm h^{-1}), the Arctic (0.8-10.6 nm h^{-1}) and a remote boreal forest (1.3 – 5 nm h^{-1}) [17].
397 The relatively lower growth rate observed at this sampling site can most likely be attributed to
398 the strong interplay between the nuclei growth and their loss by coagulation. The smaller the
399 degree of particulate pollution (smaller condensation sink), the slower small nuclei must grow
400 in order to survive the coagulational scavenging onto larger pre-existing particles [17, 46-47].
401
402 **4. Conclusions**
403 In this study, we conducted an intensive field measurement campaign of particle number
404 concentration and size distributions, together with other gaseous pollutants and
405 meteorological parameters, at a rural site in northeastern Australia. The measurements were
406 conducted during September 2006, when the average hours of sunshine per day were the
407 highest and average rainfall is at its lowest.
408 Back trajectory analysis indicated that the air masses arriving at the study site mainly
409 originated from three clusters i.e. 1, 2 and 3, including both inland and marine air (accounting
410 for 89% of the total air samples). All three clusters presented an early-morning anthropogenic
411 peak of particle concentration, which was probably due to the vehicular emissions and/or
412 cooking activities of local residences at that time. Late-morning photochemical particle
413 formation events, followed by the growth of nucleation mode particles into Aitken and
414 accumulation modes throughout the afternoon and evening, were also observed for three of
415 the four clusters (clusters 1, 3 and 4). However, the modal diameter and the concentration of
416 the newly formed particles for cluster 2 remained constant between 12:00 and 15:00, probably
417 due to the impact of high wind speed from the ocean, which allowed time for particle
418 formation but not subsequent particle growth. The night time size distribution of the three
419 major clusters was dominated by Aitken mode particles, whereas the day time size
420 distribution presented different modal structures for different air masses. The inland air
421 (cluster 1) showed a bimodal spectrum of the Aitken and accumulation modes, whereas a
422 single modal distribution was found for marine air cluster 2 and 3, with a GMD of 20.6 nm
423 and 28.9 nm, respectively.
424 In general, nucleation mode particles dominated the size distribution of the
425 photochemical event during day time, with a GMD <30 nm. This was found to be somewhat

different from the GMD generated by combustion sources, such as biomass burning, which showed a bimodal lognormal distribution, dominated by Aitken and accumulation modes. Nucleation mode particle concentrations were also found to be anti-correlated with aerosol surface area concentrations, which can be attributed to the fact that concentrations of the nucleating species decrease due to heterogeneous condensation, as pre-existing aerosol concentrations increase, resulting in a reduction in particle production rates. The average particle growth rate was also estimated by calculating the evolution of GMD for the modal mode as a function of time and was found to be 1.6 nm h^{-1}. This growth rate is lower than that observed in other polluted areas and is comparable to that observed at other clean sites.

Initial analysis of the potential precursors of photochemical formation showed good correlation between hourly average SO_2 concentration and the concentration of nucleation mode particles ($R^2 = 0.51$, $p = 0.0012$), suggesting that SO_2 products might be involved in the increased nucleation mode particle concentration observed during the photochemical event. However, more research is necessary in order to fully understand the precursors for photochemical formation of nucleation mode particles.

Acknowledgements

The field measurements were funded by the Department of Public Works, Queensland Government. The data analysis presented in this paper is supported by the Research Grants Council of the Hong Kong Special Administrative Region (Project No. PolyU 5163/07E), and the Research Grant (87PK) of the Hong Kong Polytechnic University. The technical assistance of Dr. Graham Johnson is greatly acknowledged and our thanks also go to Ms. Rachael Robinson for her editing.

References

[1] USEPA (United States Environmental Protection Agency), **1982**, Air Quality Criteria for Particulate Matter and Sulfur Oxides, *EPA/600/8-82-029a-c*, EPA, Washington, D.C.

[2] S. A. Twomey, M. Piepgrass, T. L. Wolfe, An assessment of the impact of pollution on global cloud albedo. *Tellus B* **1984**, 36, 356.

[3] B. S. Cohen, R. G. Sussman, M. Lippman, Ultrafine particle deposition in a human tracheobronchial cast. *Aerosol Sci. Technol.* **1990,** 12, 1082.

[4] R. J. Charlson, J. Langner, M. O. Andreae, S. G. Warren, Perturbation of the northern hemisphere radiative balance by backscattering from anthropogenic sulfate aerosols. *Tellus A-B* **1991**, 43, 152.

[5] R. J. Weber, J. J. Marti, P. H. McMurry, Measurements of new particle formation and ultrafine particle growth rates at a clean continental site. *J. Geophys. Res* **1997**, 102, 4375.

[6] DHCMEAP (Department of Healths Committee on the Medical Effects of Air Pollutants), **1995,** Non-Biological Particles and Health. HMSO, London.

[7] G. McFiggans, P. Artaxo, U. Baltensperger, H. Coe, M. C. Facchini, G. Feingold, S. Fuzzi, M. Gysel, A. Laaksonen, U. Lohmann, T. F. Mentel, D. M. Murphy, C. D. O'Dowd, J. R. Snider, E. Weingartner, The effect of physical and chemical aerosol properties on warm cloud droplet activation. *Atmos. Chem. Phys*. **2006**, 6, 2593

[8] S. Kreidenweis, G. Tyndall, M. Barth, F. Dentener, J. Lelieveld, M. Mozurkewich, in *Atmospheric Chemistry and Global Change* (Eds G. P. Brasseur, J. J. Orlando, G. S. Tyndall) **1999**, pp. 117-154 (Oxford University Press: New York).

[9] F. Stratmann, H. Siebert, G. Spindler, B. Wehner, D. Althausen, J. Heintzenberg, O. Hellmuth, R. Rinke, U. Schmieder, C. Seidel, T. Tuch, U. Uhrner, A. Wiedensohler, U. Wandinger, M. Wendisch, D. Schell, A. Stohl, New-particle formation events in a continental boundary layer: first results from the SATURN experiment. *Atmos.Chem.Phys.* **2003**, 3, 1445.

[10] J. H. Seinfeld, S. N. Pandis, *Atmospheric Chemistry and Physics: From air pollution to climate change*, *2nd edn* **2006** (John Wiley & Sons: New Jersey).

[11] B. J. Finlayson-Pitts, J. N. Finlayson-Pitts, Jr., *Chemistry of the Upper and Lower Atmosphere: Theory, Experiments and applications* **2000** (Academic Press: Orlando, FL).

[12] A. Wiedensohler, D. S. Covert, E. Swietlicki, P. Aalto, J. Heintzenberg, C. Leck, Occurrence of an ultrafine particle mode less than 20 nm in diameter in the marine boundary layer during Arctic summer and autumn. *Tellus B* **1996**, 48, 213.

[13] J. M. Mäkelä, I. K. Koponen, P. Aalto, M. Kulmala, One-year data of submicrometer size modes of tropospheric background aerosol in southern Finland. *J. Aerosol Sci.* **2000**, 31, 595.

[14] K. Park, J. Y. Park, J.-H. Kwak, G. N. Cho, J. –S. Kim, Seasonal and diurnal variations of ultrafine particle concentration in urban Gwangju, Korea: Observation of ultrafine particle events. *Atmos. Environ.* **2008**, 42, 788.

[15] L. Shang, M. Hu, Z. Wu, B. Wehner, A. Wiedensohler, Y. Cheng, Aerosol number size distribution and new particle formation at a rural/coastal site in Pearl River Delta (PRD) of China. *Atmos. Environ.* **2008**, doi: 10.1016/j.atmosenv.2008.01.063

[16] M. Kulmala, I. Riipinen, M. Sipila, H.E. Manninen, T. Petaja, H. Junninen, M. Dal Maso, G. Mordas, A. Mirme, M. Vana, A. Hirsikko, L. Laakso, R. M. Harrison, I. Hanson, C. Leung, K. E. J. Lehtinen, V.-M. Kerminen, Toward direct measurement of atmospheric nucleation. *Science* **2007**, 318, 89

[17] M. Kulmala, T. Petäjä, P. Mönkkönen, I. K. Koponen, M. Dal Maso, P. P. Aalto, K. E. J. Lehtinen, V.-M. Kerminen, On the growth of nucleation mode particles: source rates of condensable vapor in polluted and clean environments. *Atmos. Chem. Phys.* **2005**, 5, 409.

[18] D. S. Covert, A. Wiedensohler, P. Aalto, J. Heintzenberg, P. H. McMurry, C. Leck, Aerosol number size distributions from 3 to 500 nm diameter in the Arctic marine boundary layer

during summer and autumn. *Tellus B* **1996**, 48, 197.
[19] R. J. Weber, P. H. McMurry, F. L. Eisele, D. J. Tanner, Measurement of expected nucleation precursor species and 3 to 500 nm diameter particles at Mauna Loa Observatory, Hawaii. *J. Atmos. Sci.* **1995**, 52, 2242.
[20] R. J. Weber, P. H. McMurry, Fine particle size distributions at the Manua Loa Observatory, Hawaii. *J. Geophys. Res.* **1996**, 101, 14767.
[21] J. M. Mäkelä, P. Aalto, V. Jokinen, T. Pohja, A. Nissinen, S. Palmroth, T. Markkanen, K. Seitsonen, H. Lihavainen, M. Kulmala, Observations of ultrafine aerosol particle formation and growth in boreal forest. *Geophys. Res. Lett.* **1997**, 24, 1219.
[22] J. M. Mäkelä, M. D. Maso, L. Pirjora, P. Keronen, L. Laakso, M. Kulmala, A. Laaksonen, Characteristics of the atmospheric particle formation events observed at a borel forest site in southern Finland. *Boreal Environ. Res.* **2000**, 5, 299.
[23] M. Kulmala, A. Toivonen, J. M. Mäkelä, A. Laaksonen, Analysis of the growth of nucleation mode particles in Boreal Forest. *Tellus B* **1998**, 50, 449.
[24] M. Kulmala, K. Hämeri, P. Aalto, J. M. Mäkelä, L. Pirjola, E. D. Nilsson, G. Buzorius, Ü. Rannik, M. Dal Maso, W. Seidl, T. Hoffman, R. Janson, H.-C. Hansson, Y. Viisanen, A. Laaksonen, C. D. O'Dowd, Overview of the international project on biogenic aerosol formation in the boreal forest (BIOFOR). *Tellus B* **2001,** 53, 324.
[25] K. S. Woo, D. R. Chen, D. Y. H. Pui, P. H. McMurry, Measurement of Atlanta aerosol size distributions: observations of ultrafine particle events. *Aerosol Sci. Technol.* **2001**, 34, 75.
[26] C. O. Stanier, A. Y. Khlystov, S. N. Pandis, Nucleation events during the Pittsburgh air quality study: description and relation to key meteorological, gas phase, and aerosol parameters. *Aerosol Sci. Technol.* **2004**, 38, 253.
[27] J. G. Watson, J. C. Chow, K. Park, D. H. Lowenthal, Nanoparticle and ultrafine particle events at the Fresno supersite. *J. Air Waste Manage. Assoc.* **2006**, 56, 417.
[28] T. Suni, M. Kulmala, A. Hirsikko, T. Bergman, L. Laakso, P. P. Aalto, R. Leuning, H. Cleugh, S. Zegelin, D. Hughes, E. van Gorsel, M. Kitchen, M. Vana, U. Hŏrrak, S. Mirme, A. Mirme, S. Sevanto, J. Twining, C. Tadros, Formation and characteristics of ions and charged aerosol particles in a native Australian Eucalypt forest. *Atmos. Chem. Phys.* **2008**, 8, 129
[29] S. I. Jimi, J. L. Gras, S. T. Siems, P. B. Krummel, A short climatology of nanoparticles at the Cape Grim Baseline Air Pollution Station, Tasmania. *Environ. Chem.* **2007**, 4, 301
[30] Australian Bureau of Statistics, *2006 Census QuickStats: Brisbane*, **2007**, Statistical Division, Australian Bureau of Statistics.
[31] Bureau of Meteorology, http://www.bom.gov.au/climate/averages/tables/cw_040223.shtml, **2008**, Bureau of Meteorology, Australian Government.
[32] P. A. Baron, K. Willeke, *Aerosol Measurement: Principles, Techniques and Applications* **2001** (John Wiley and Sons: New York).
[33] W. Birmili, A. Wiedensohler, New particle formation in the continental boundary layer: meteorological and gas phase parameter influence. *Geophys. Res. Lett.* **2000**, 27, 3325.
[34] R. J. Weber, P. H. McMurry, R. L. III Mauldin, D. J. Tanner, F. L. Eisele, A. D. Clarke, V. N. Kapustin, New particle formation in the remote troposphere: a comparison of observations at various sites. *Geophys. Res. Lett.* **1999,** 26, 307.

[35] C. D. O'Dowd, G. McFiggans, D. J. Creasey, L. Pirjola, C. Hoell, M. H. Smith, B. J. Allan, J. M. C. Plane, D. E. Heard, J. D. Lee, M. J. Pilling, M. Kulmala, On photochemical production of biogenic new particles in the coastal boundary layer. *Geophys. Res. Lett.* **1999**, 26, 1707.

[36] L. Morawska, S. Thomas, N. Bofinger, D. Wainwright, D. Neale, Comprehensive characterization of aerosols in a subtropical urban atmosphere: Particle size distribution and correlation with gaseous pollutants. *Atmos. Environ*. **1998**, 32, 2467.

[37] S. Henning, E. Weingartner, S. Schmidt, M. Wendisch, H. W. Gäggeler, U. Baltensperger, Size-dependent aerosol activation at the high-alpine site Jungfraujoch (3580 m asl). *Tellus B* **2002**, 54, 82.

[38] M. Komppula, M. Dal Maso, H. Lihavainen, P. P. Aalto, M. Kulmala, Y. Viisanen, Comparision of new particle formation events at two locations in northern Finland. *Boreal Environ. Res.* **2003**, 8, 395.

[39] M. Dal Maso, L. Sogacheva, P. P. Aalto, I. Riipinen, M. Komppula, P. Tunved, L. Korhonen, V. Suur-Uski, A. Hirsikko, T. Kurtén, V.-M. Kerminen, H. Lihavainen, Y. Viisanen, H.-C. Hansson, M. Kulmala, Aerosol size distribution measurements at four Nordic field stations: identification, analysis and trajectory analysis of new particle formation bursts. *Tellus B*, **2007**, 59, 350.

[40] L. Laakso, H. Laakso, P. P. Aalto, P. Keronen, T. Petäjä, T. Nieminen, T. Pohja, E. Siivola, M. Kulmala, N. Kgabi, M. Molefe, D. Mabaso, D. Phalatse, K. Pienaar, V.-M. Kerminen, Basic characteristics of atmospheric particles, trace gases and meteorology in a relatively clean Southern African Savannah environment. *Atmos. Chem. Phys.* **2008**, 4823-4839

[41] R. Griffin, D. Cocker III, J. Seinfeld, D. Dabdub, Estimate of global atmospheric organic aerosol from oxidation of biogenic hydrocarbons. *Geophys. Res. Lett.* **1999**, 26, 2721.

[42] M. Boy, M. Kulmala, T. M. Ruuskanen, M. Pihlatie, A. Reissell, P. P. Aalto, P. Keronen, M. Dal Maso, H. Hellen, H. Hakola, R. Jansson, M. Hanke, F. Arnold, Sulfuric acid closure and contribution to nucleation mode particle growth. *Atmos. Chem. Phys. Discussion* **2004**, 4, 6341.

[43] J. J. Marti, R. J. Weber, P. H. McMurry, New particle formation at a remote continental site: Assessing the contributions of SO2 and organic precursors. *J. Geophys. Res.* **1997,** 102, 6331.

[44] M. R. Stolzenburg, P. H. McMurry, H. Sakurai, J. N. Smith, R. L. Mauldin, F. L. Eisele, C. F. Clement, Growth rates of freshly nucleated atmospheric particles in Atlanta. *J. Geophys. Res.* **2005**, 110, D22S05.

[45] S. Qian, H. Sakurai, P. H. McMurry, Characteristics of regional nucleation events in urban East St. Louis. *Atmos. Environ.* **2007**, 41, 4119.

[46] V.-M. Kerminen, L. Pirjola, M. Kulmala, How significantly does coagulation scavenging limit atmospheric particle production? *J. Geophys. Res.* **2001**, 106, 24119.

[47] M. Kulmala, H. Vehkamäki, T. Petäjä, M. Dal Maso, A. Lauri, V.-M. Kerminen, W. Birmili, P. H. McMurry, Formation and growth rates of ultrafine atmospheric particles: a review of observations. *J. Aerosol Sci.* **2004**, 35, 143.

590 **Captions**

591 **Table 1** Average particle number concentration and the time with the maximum value for
592 each of the three modes in each cluster air mass

593 **Figure 1** (a) Map showing the sampling site and surrounding environments; (b) Averaged
594 pathways of 48-hour back trajectory based on cluster analysis. The background map in 1(a)
595 gives the biogenic emission rate of VOC, (data from Environmental Protection Agency of
596 Queensland Government, http://www.epa.qld.gov.au/register/p00873ak.pdf). Markers on
597 trajectories show hourly and 3-hourly location in Figs 1a and 1b, respectively.

598 **Figure 2** Contour plots of the average diurnal variations of particle size distribution for the
599 three classified air masses, and diurnal patterns of the meteorological data and the
600 concentrations of airborne pollutants

601 **Figure 3** Diurnal patterns of the particle size distributions of the three classified air masses

602 **Figure 4** Contour plot of photochemical formation of particles and growth on 20 September
603 2006. Color represents dN/dlnDp (cm^{-3})

604 **Figure 5** Size distributions of photochemical formation and biomass burning

605 **Figure 6** Geometric mean diameter (GMD) of nucleation mode particles as a function of time
606 during the photochemical event on 20 September 2006: calculating particle growth rate

607
608
609
610
611
612
613
614
615
616
617
618
619
620
621
622
623
624

Table 1

Air mass type	Nucleation mode (15-30nm)		Aitken mode (30-100nm)		Accumulation mode (100nm-737nm)	
	Average concentration (Standard Deviation)	Timing of Max. value (Local Time)	Average concentration (Standard Deviation)	Timing of Max. value (Local Time)	Average concentration (Standard Deviation)	Timing of Max. value (Local Time)
Cluster1	1454 (1347)	12:45	4137 (2022)	1:45	1547 (1870)	--[a]
Cluster2	959 (574)	12:45	1201 (547)	22:15	263 (317)	--
Cluster3	1129 (644)	12:45	2428 (1356)	23:45	710 (1025)	--

[a] No obvious accumulation mode for the three clusters was observed

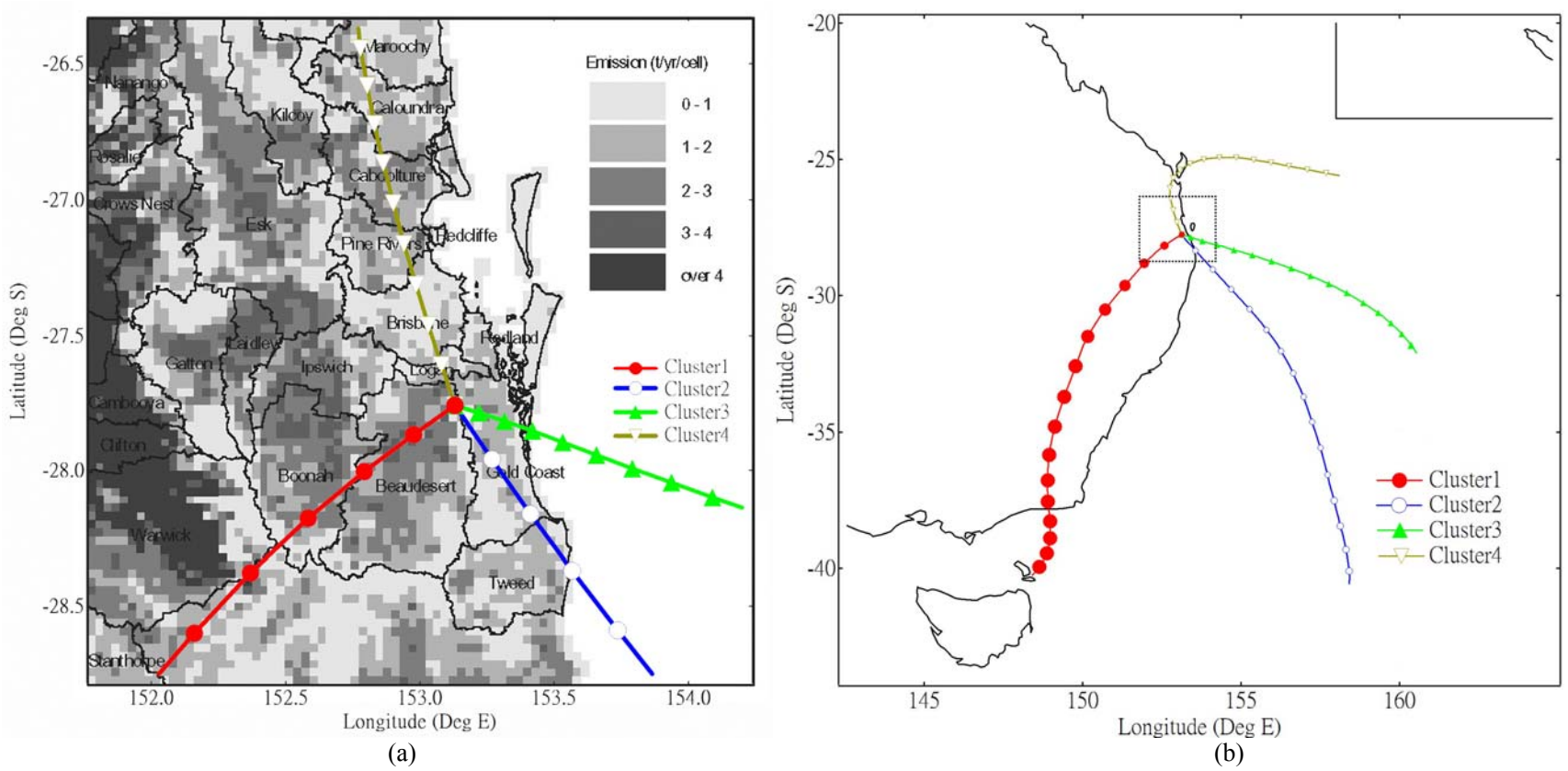
Emission (t/yr/cell)
0 - 1
1 - 2
2 - 3
3 - 4
over 4
Cluster1
Cluster2
Cluster3
Cluster4
Maroochy
Caloundra
Kilcoy
Caboolture
Esk
Redcliffe
Brisbane
Redland
Ipswich
Logan
Gold Coast
Boonah
Beaudesert
Tweed
Warwick
Stanthorpe
Latitude (Deg S)
Longitude (Deg E)
-26.5
-27.0
-27.5
-28.0
-28.5
152.0
152.5
153.0
153.5
154.0
-20
-25
-30
-35
-40
145
150
155
160

(a) (b)

Figure 1

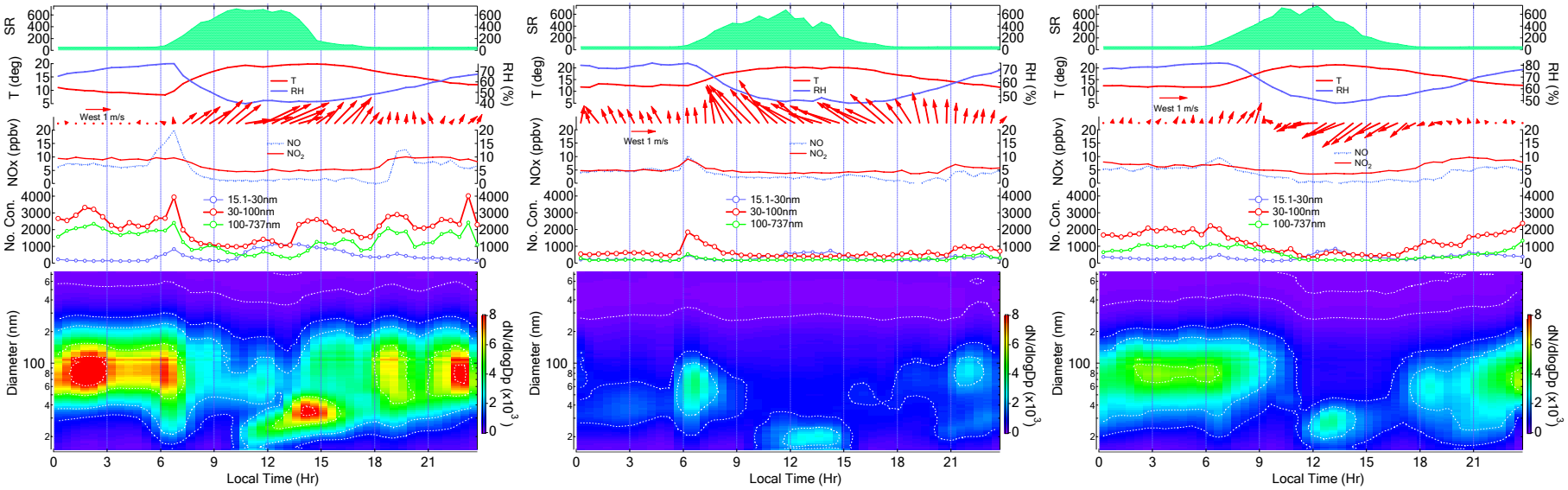

Cluster 1 – Inland Air

Cluster 2 –Marine Air

Cluster 3 – Marine plus Local Air

Figure 2

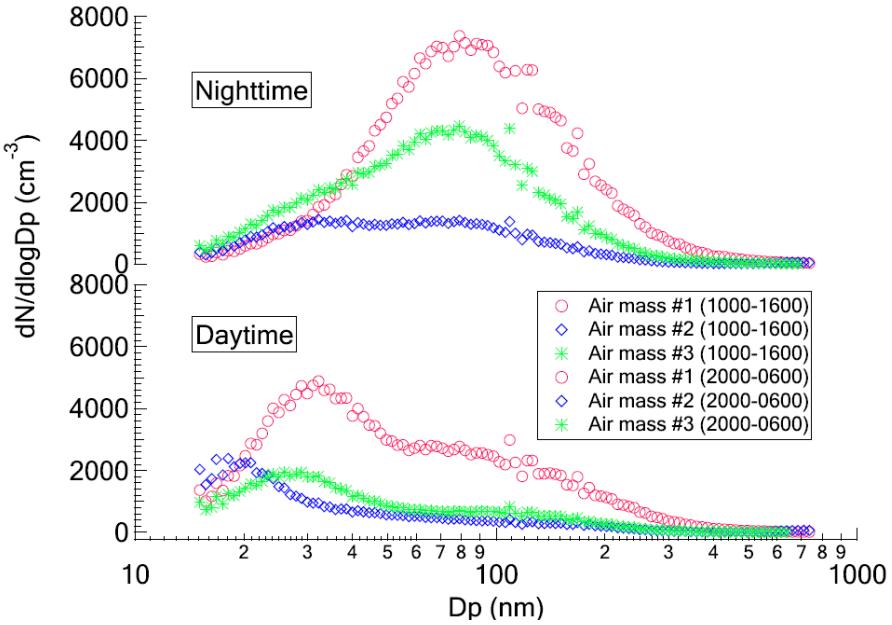

Figure 3

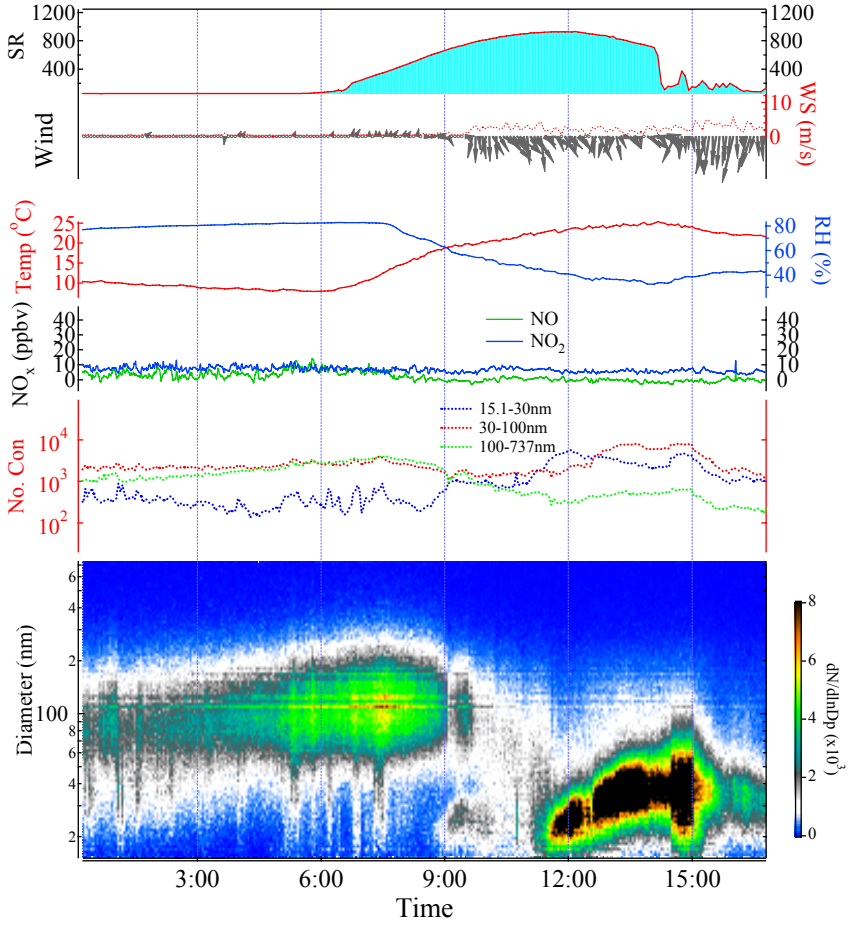

Figure 4

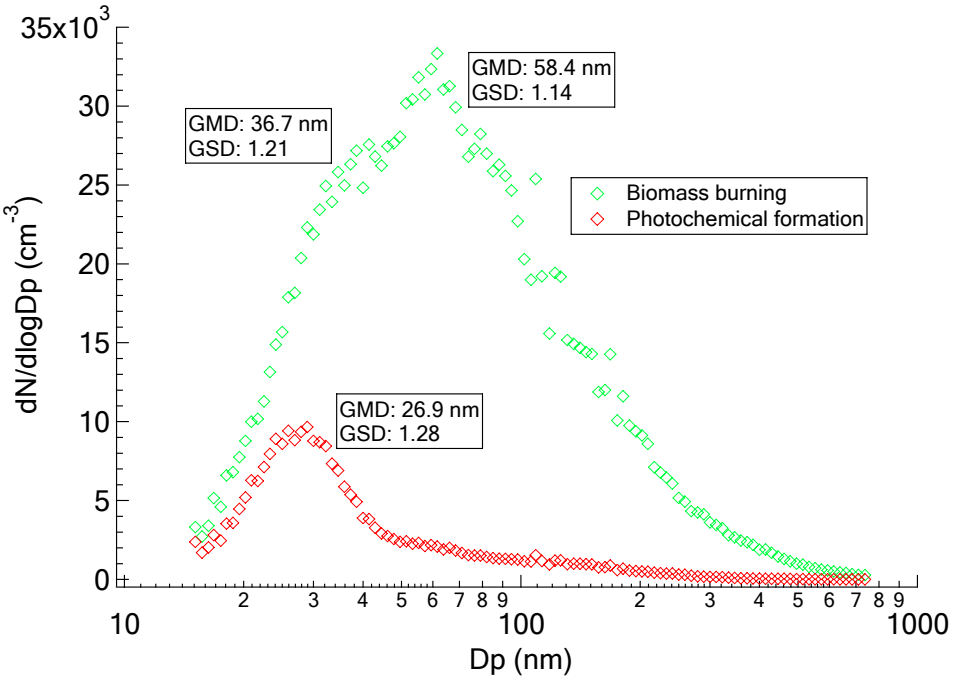

Figure 5

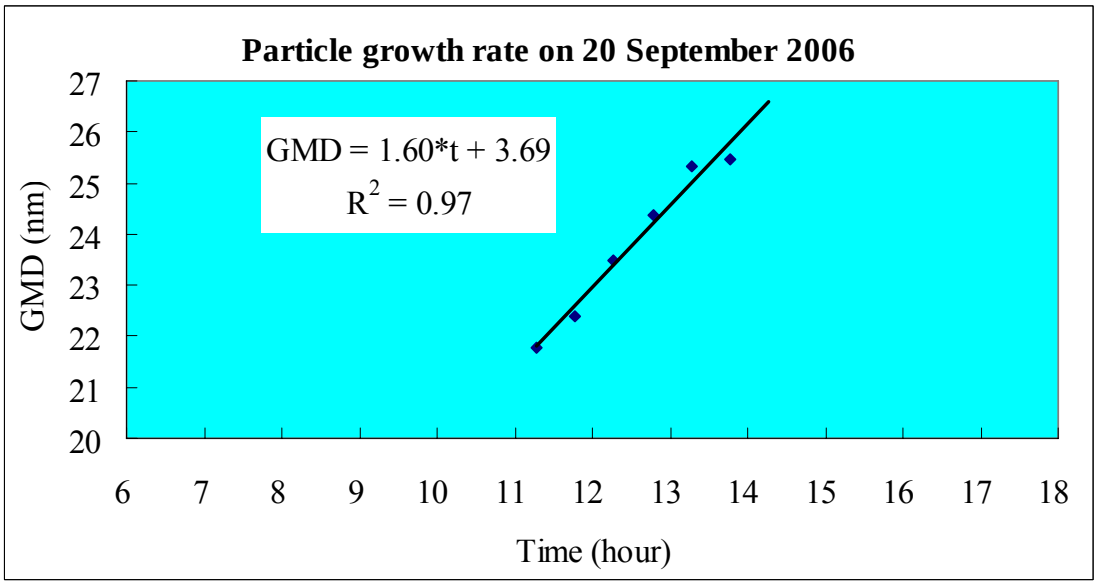

Figure 6